Supporting Information

Superelastic Carbon Aerogel with Ultrahigh and Wide-range Linear Sensitivity

Yijie Hu[1], Hao Zhuo[1], Zehong Chen[1], Kunze Wu[1], Qingsong Luo[1], Qingzhong Liu[1], Shuangshuang Jing[1], Chuanfu Liu[1], Linxin Zhong[1,*], Runcang Sun[2,*], and Xinwen Peng[1,*]

[1] State Key Laboratory of Pulp and Paper Engineering, South China University of Technology, Guangzhou, 510641, China.

[2] Centre for Lignocellulose Science and Engineering and Liaoning Key Laboratory Pulp and Paper Engineering, Dalian Polytechnic University, Dalian 116034, China.

* Corresponding authors. E-mail: lxzhong0611@scut.edu.cn (L. Zhong), rcsun3@bjfu.edu.cn (R. Sun), and fexwpeng@scut.edu.cn (X. Peng)

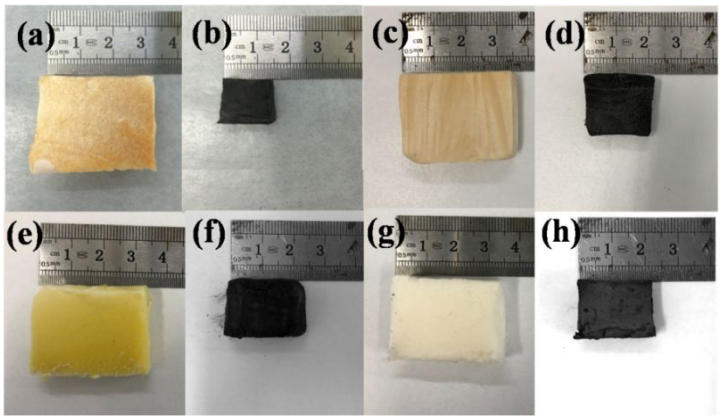

Figure S1. Pictures of as-prepared aerogels and carbon aerogels. Photographs of a) Fe-CS, b) Fe-CS-C, c) Fe-CS/CNC, d) Fe-CS/CNC, e) Fe-CNC, f) Fe-CNC-C, g) HAC-CS/CNC, and h) HAC-CS/CNC-C, respectively.

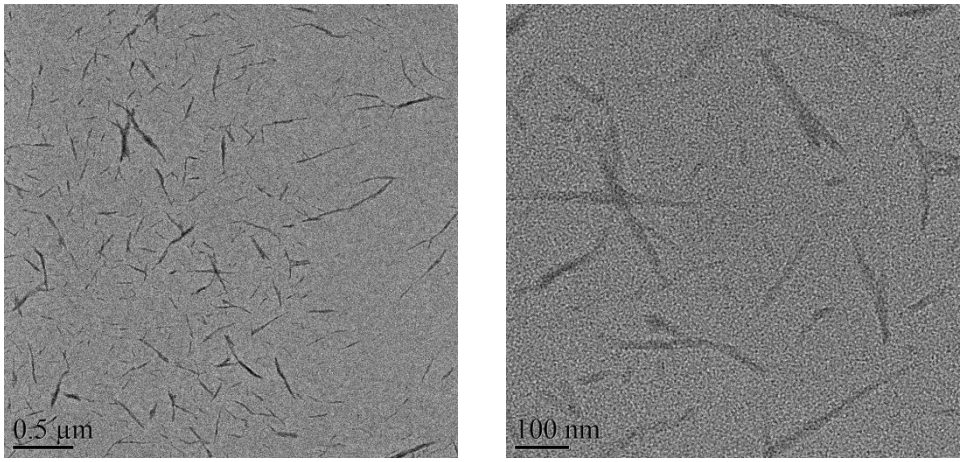

Figure S2. TEM images of CNC.

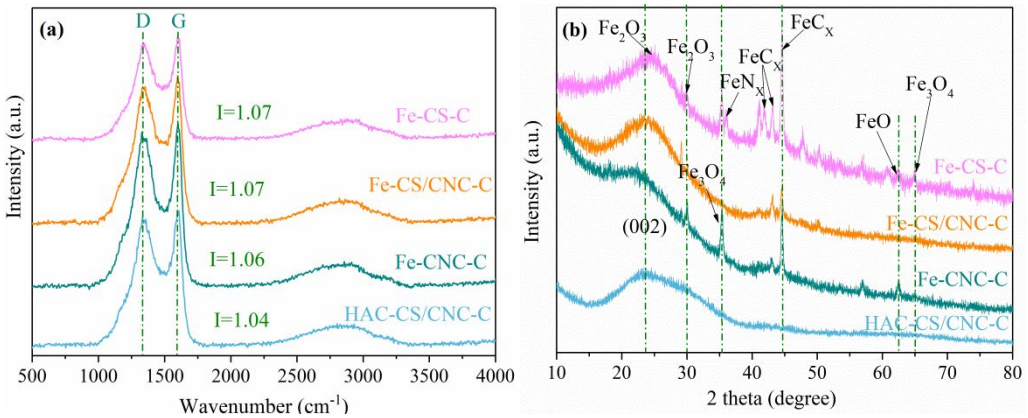

Figure S3. a) Raman and b) XRD patterns of Fe-CS-C, Fe-CNC-C, Fe-CS/CNC-C, and HAC-CS/CNC-C, respectively.

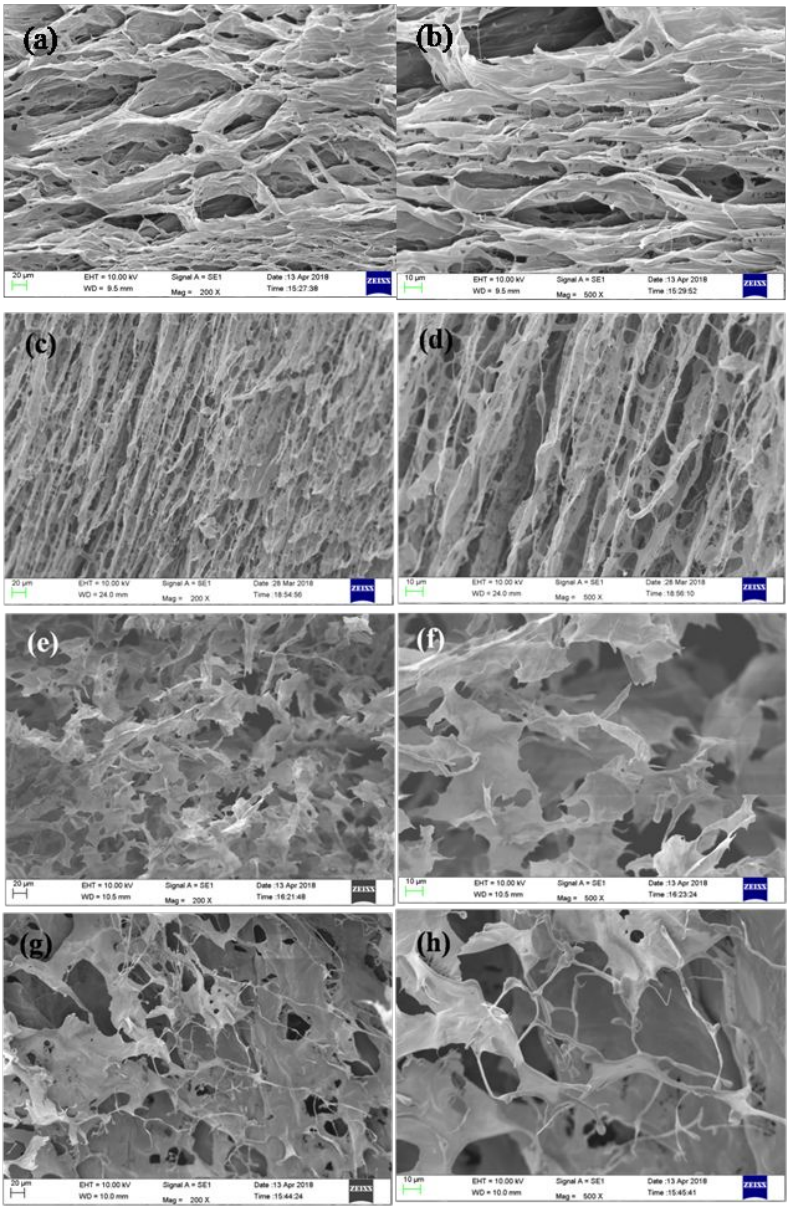

Figure S4. SEM images of a, b)Fe-CS, c, d) Fe-CS/CNC, e, f) Fe-CNC, and g, h) HAC-CS/CNC, respectively.

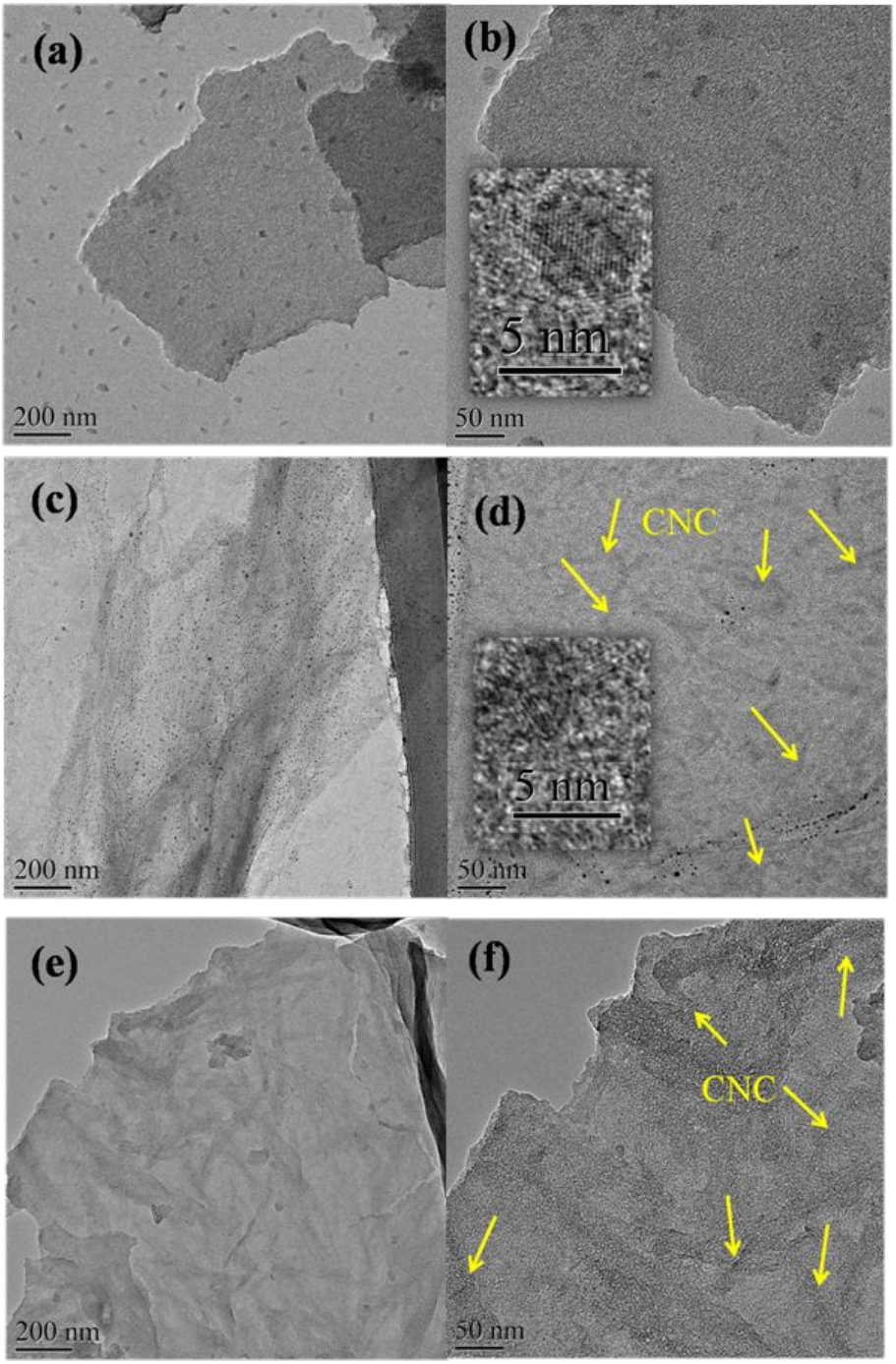

Figure S5. TEM images of a, b) Fe-CS-C, c, d) Fe-CS/CNC-C, and e, f) HAC-CS/CNC-C.

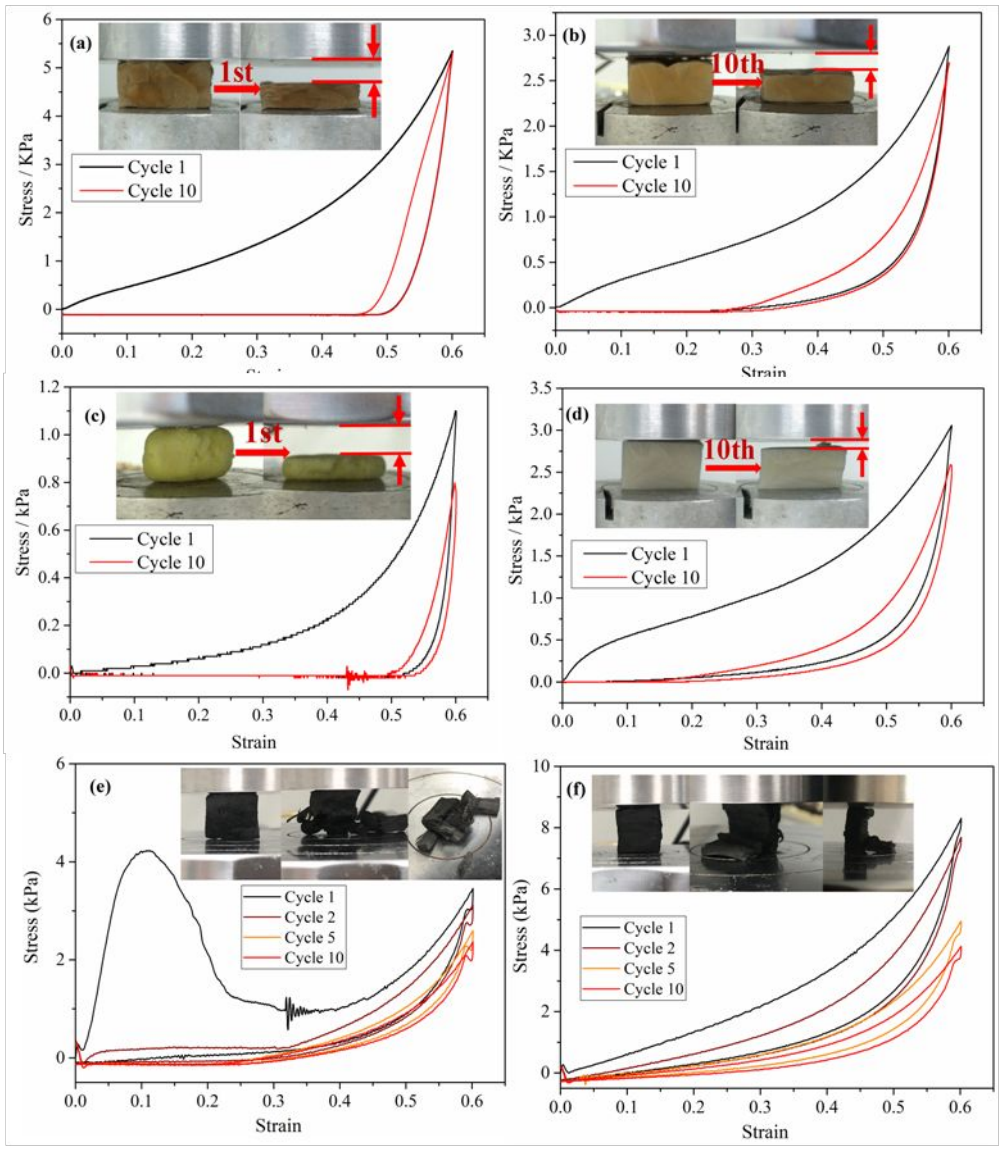

Figure S6. Stress-strain plots of a) Fe-CS, b) Fe-CS/CNC, c) Fe-CNC, and d) HAC-CS/CNC, respectively. Stress-strain plots from front (e) and side direction (f), respectively.

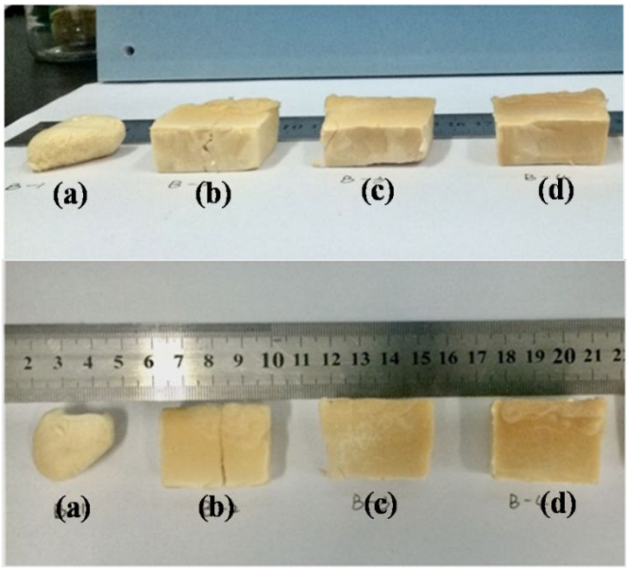

Figure S7. Pictures of Fe-CS/CNC with different $FeCl_3$ concentrations: a) Fe_1-CS/CNC, b) Fe_3-CS/CNC, c) Fe_5-CS/CNC, and d) Fe_7-CS/CNC, respectively.

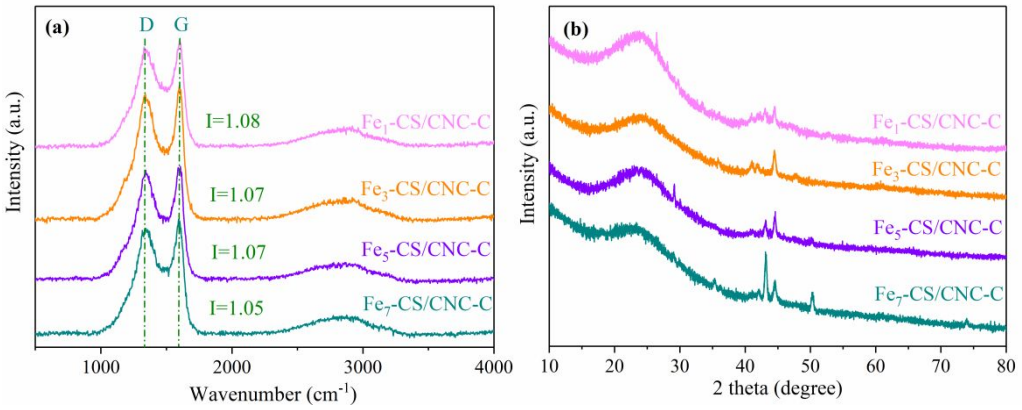

Figure S8. a) Raman and b) XRD patterns of Fe_1-CS/CNC-C, Fe_3-CS/CNC-C, Fe_5-CS/CNC-C, and Fe_7-CS/CNC-C, respectively.

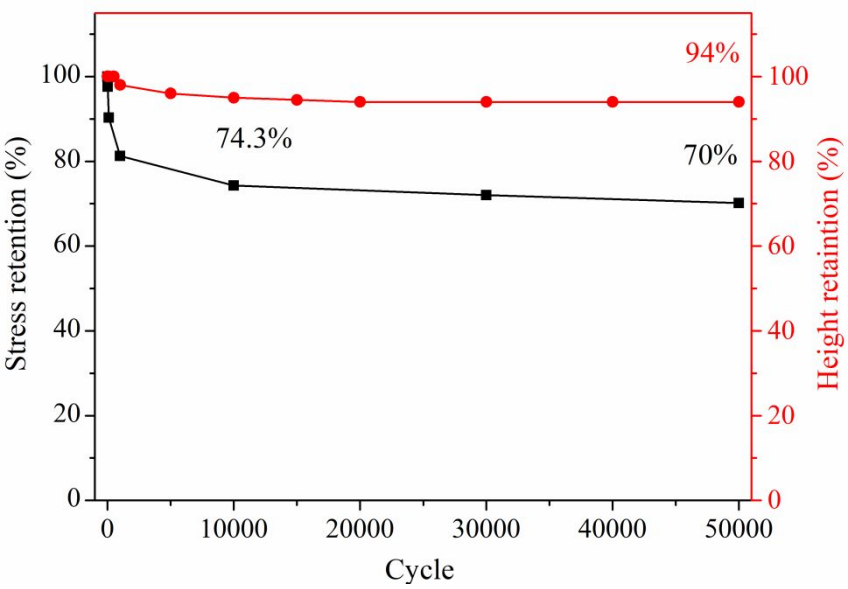

Figure S9. Height and stress retentions of Fe_5-CS/CNC-C for 50000 cycles at 50% strain.

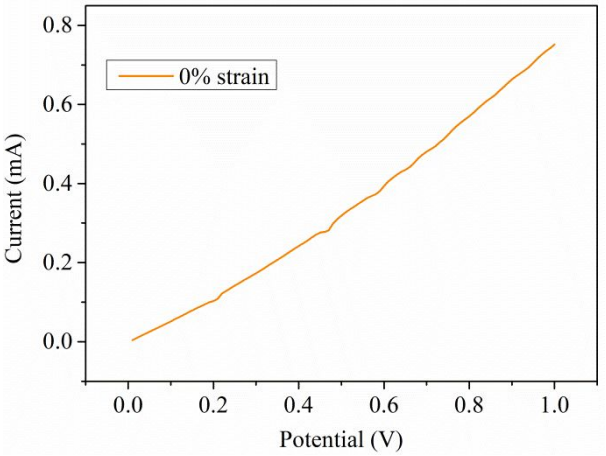

Figure S10. The current versus voltage curve at 0% strain.

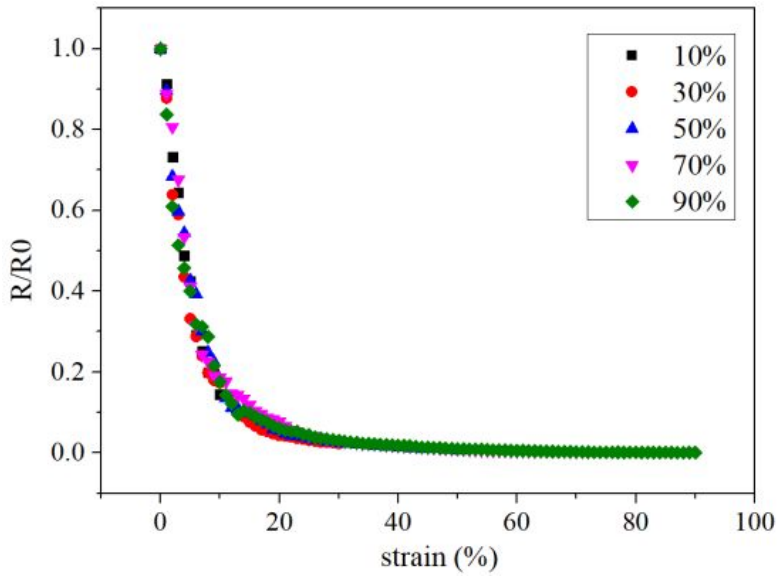

Figure S11. The normalized resistances of Fe_5-CS/CNC-C at different strains.

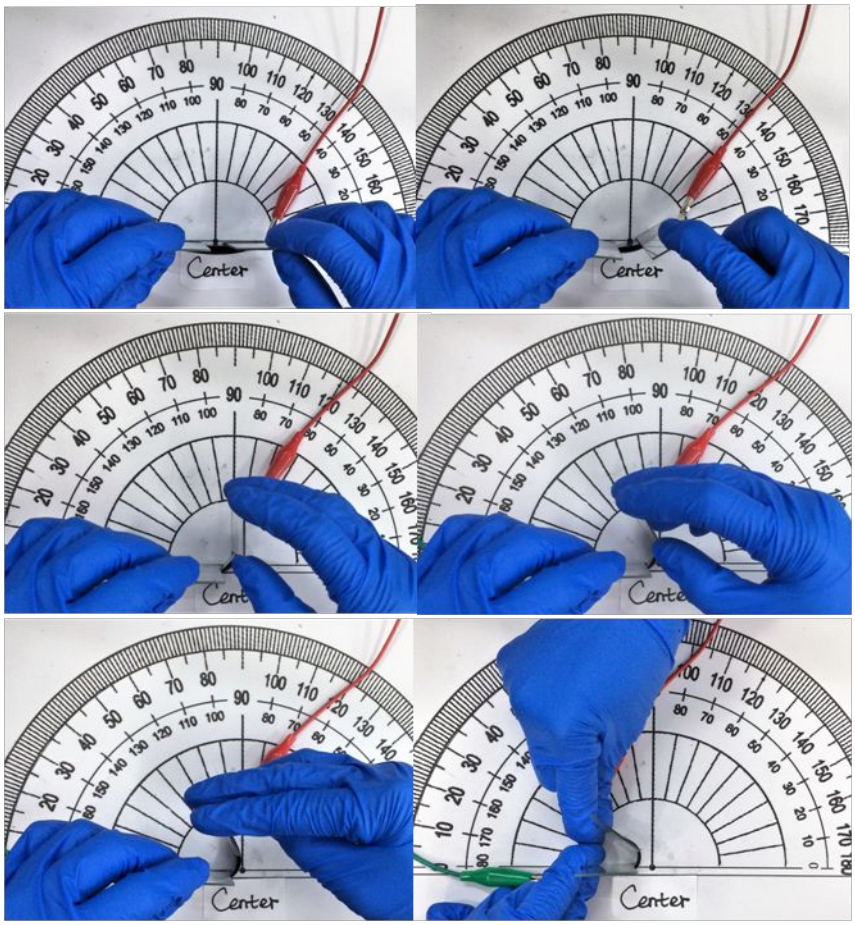

Figure S12. Bending Fe_5-CS/CNC-C with different angles.

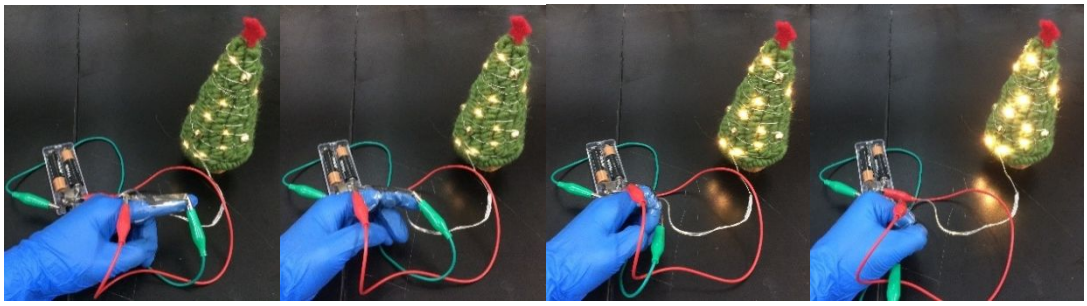

Figure S13. LED responses at different bending degrees.

Table S1. Densities of the as-prepared carbon aerogels.

Samples	Fe-CS-C	Fe_5-CS/CNC-C	Fe-CNC-C	HAC-CS/CNC-C
Density (mg/cm^3)	56.7	17.5	9.2	16.6

Table S2. Height retentions of carbon aerogels with different $FeCl_3$ concentrations at 50% strain.

Cycles	10	100	500	1000
Fe_1-CS/CNC-C	66.7%	-	-	-
Fe_3-CS/CNC-C	95%	90%	89%	89%
Fe_5-CS/CNC-C	100%	100%	100%	99%
Fe_7-CS/CNC-C	100%	99%	98%	98%

Table S3. Stress retentions of carbon aerogels with different $FeCl_3$ concentrations at 50% strain.

Cycles	10	100	500	1000
Fe_1-CS/CNC-C	53.4%	-	-	-
Fe_3-CS/CNC-C	96%	90.4%	84.3%	84.0%
Fe_5-CS/CNC-C	97.6%	90.3%	84.2%	83.0%
Fe_7-CS/CNC-C	93.7%	90.4%	86.3%	78.2%

Table S4. Fatigue resistance of different sorts of compressible aerogels.

Materials	Max strain	Cycles	Strain	Height retention	Reference
CNT foams	98%	1000	95%	-	6
Graphene aerogel	90%	1000	50%	-	28
Graphene aerogels	50%	10	50%		29
Graphene aerogel spheres	95%	1000	70%	-	30
Graphene aerogel	95%	10	95%	-	31
Graphene aerogel	90%	50	80%	-	32
Graphene aerogel	80%	20	50%	-	33
rGO aerogel	99%	10000	50%		18
rGO aerogel	90%	250000	50%	98%	17
GO aerogel	50%	1000	50%	92%	27
GO aerogel	90%	10	90%	95%	34
Graphene-coated SWCNT aerogels	80%	2000	60%	-	14
Graphene-coated SWCNT aerogels	40%	10000	~30%	-	16
Wood-derived carbon aerogel	80%	10000	50%	-	36
Carbon aerogel	80%	1000	60%	-	37
RF/GO aerogel	80%	100	50%	88.6%	35
Chitosan + CNC	95%	50000	50%	94%	This work
		300	70%	90%	